

## THE CONTRIBUTION OF INCREASED INCOMING SHORTWAVE RADIATION TO THE RETREAT OF THE RWENZORI GLACIERS, EAST AFRICA, DURING THE 20TH CENTURY

THOMAS MÖLG,\* CHRISTIAN GEORGES and GEORG KASER

*Tropical Glaciology Group, Department of Geography, University of Innsbruck, Austria*

*Received 22 February 2002*

*Revised 6 November 2002*

*Accepted 6 November 2002*

### ABSTRACT

Based on (i) the observation of spatially differential glacier retreats in the tropical Rwenzori Range (East Africa) during the 20th century, which are most striking on the mountains Baker and Speke, and (ii) the information on an abrupt climate change to drier conditions in East Africa at the end of the 19th century, the following hypothesis is derived: owing to a drier atmosphere than in a previous period, both accumulation (possibly supported by increasing air temperatures) and convective cloud activity have decreased. Consequently, increased incoming shortwave radiation, especially during the morning hours, induced a differentially increased ablation that could not be compensated by mass advection on the mountains Baker and Speke.

The results obtained from a combined radiation–terrain model, run for one more humid and one drier climatic scenario, confirm the hypothesis by quantifying the correlation between increased incoming shortwave radiation and glacier surface area loss. In the context of modern climate fluctuations, the results are a further indicator for a drastic climatic dislocation in East Africa at the end of the 19th century, leaving a humid regime behind and leading to a relatively dry regime, which is forcing the recession of glaciers not only by less accumulation but also by less protection against shortwave radiation through clouds. Copyright © 2003 Royal Meteorological Society.

KEY WORDS: tropical glaciers; East Africa; Rwenzori; climatic change; radiation modelling; shortwave radiation

### 1. INTRODUCTION

In the thermally homogeneous atmosphere of the tropics, the reaction of glaciers to climate represents a particularly sensitive interaction and deserves special attention in the context of understanding global climate changes (e.g. Hastenrath, 1995; Kaser *et al.*, 1996; Kaser, 2001; Wagnon *et al.*, 2001). Glaciers in low latitudes still exist in New Guinea, in Equatorial East Africa, and in the South American Andes. After the latest maximum extent around the mid and second half of the 19th century they all have suffered drastic ice wastage (Kaser, 1999). For the three glaciated massifs in East Africa (Mount Kenya, Rwenzori,<sup>1</sup> and Kilimanjaro), this was comprehensively reported by Hastenrath (1984). Specific details for Mount Kenya are provided by Hastenrath and coworkers (Krus and Hastenrath, 1987; Hastenrath, 1989; Hastenrath *et al.*, 1989), for the Rwenzori by Kaser and coworkers (Kaser and Nogler, 1991, 1996; Kaser and Osmaston, 2002), and for Kilimanjaro by Hastenrath and Greischar (1997) and Thompson *et al.* (2002). Decreased precipitation and increasing temperature, and, therefore, a higher position of the lower snow fall limit, are regarded as dominating reasons for the generally strong glacier recession in Equatorial East Africa (Krus and Hastenrath, 1987; Kaser and Nogler, 1996). Furthermore, changes in availability of shortwave radiation due to changes in cloudiness might also contribute to East African glacier retreats; this is supported by the analysis of Kruss

\* Correspondence to: Thomas Mölg, Tropical Glaciology Group, Department of Geography, University of Innsbruck, Innrain 52, A-6020 Innsbruck, Austria; e-mail: thomas.moelg@uibk.ac.at

and Hastenrath (1987) for Mount Kenya, and is also taken into consideration by Kaser and Nogler (1991, 1996) as one possible reason for the retreat of the Rwenzori glaciers.

The large-scale circulation over Equatorial East Africa is characterized by a double passage of the near-equatorial low-pressure trough, also known as the intertropical convergence zone (ITCZ), around April–May and September–October, northeasterly trade winds in the boreal winter, and southwesterly monsoons in the boreal summer. Trade winds and monsoonal flow, in general, bring drier conditions for the Equatorial East African region, whereas the passage of the low-pressure trough leads to stronger convective activity and moist conditions (Griffiths, 1972; Weischet and Endlicher, 2000). In the Rwenzori Range, the two rainy seasons last from March to May and from August to December. The two drier seasons in January–February and June–July are moderately pronounced because the Rwenzori is influenced by moisture advection from the interior of the continent in these months (Whittow, 1960). The altitudinal belt of maximum rainfall with an amount of *ca* 2500 mm year<sup>-1</sup> is found between 1500 and 3500 m. Precipitation decreases towards the peak regions, but values still remain >1000 mm year<sup>-1</sup> (Osmaston, 1989). Measurements of air temperature are rare in the Rwenzori mountains. The efforts of Osmaston (1989), who collected all the information about temperature in the Rwenzori Range, at least make it possible to give the altitude of the mean annual 0°C isothermal surface. Based on data from *ca* 1900–60, it was located between 4600 and 4700 m. The weather in the higher reaches of the massif is strongly controlled by the local, diurnal circulation, which is characteristic for tropical mountains (Figure 1) and was first described by Troll and Wien (1949) and more recently by Hastenrath (1991). Through the night into the early morning hours, the mountains are surrounded by sinking air masses causing clear skies in the peak regions and cloud cover over the basins where the winds converge. The rising of the sun and increasing heating of the surfaces reverse the topographically induced circulation, leading to convective cloudiness and precipitation over the mountains. This starts on the eastern slopes in the morning hours and culminates all over the massif in the afternoon. Consequently, the western slopes receive less sunshine and more precipitation. Both effects cause the glaciers to extend to lower elevations on the western slopes.

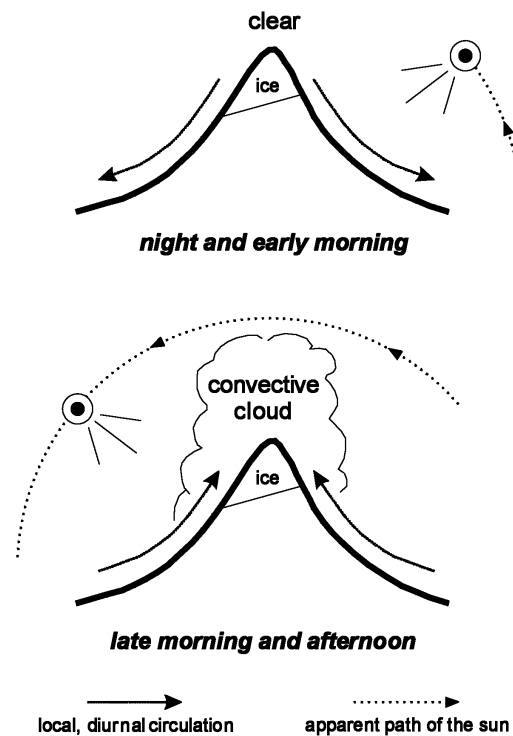


Figure 1. Scheme of diurnal circulation and cloudiness on tropical mountains. Night and early morning (top), late morning and afternoon (bottom); (after Troll and Wien (1949) and Hastenrath (1991))

According to climatic proxy data presented by Kruss (1983, 1984), Hastenrath (1984, 2001), Nicholson *et al.* (2000), and Nicholson and Yin (2001), the climatic evolution of East Africa over the past 150 years is characterized by a drastic dislocation around 1880, when lake levels dropped significantly and glaciers started to recede from a maximum extent. The relatively dry climate was maintained throughout the 20th century. Comparatively speaking, the couple of decades preceding 1880 were very humid: lakes stood high, mountain glaciation was extensive, and precipitation abundant. In contrast to this switch in humidity, there is no evidence of an abrupt change in air temperature. This marked climatic change around 1880 has led us to define two scenarios in this study (Section 3), each referring to one of the climatic regimes described. They are then correlated to the changes in glaciation.

## 2. THE OBSERVED PHENOMENA AND A HYPOTHESIS

As reported by Kaser and Osmaston (2002), the long-term variations in ice cover in the Central Rwenzori Range ( $0^\circ$ ,  $30^\circ\text{E}$ , 5109 m), which consists of the glaciated mountains Speke, Baker, and Stanley, are presented in Figure 2. It maps the reconstructed glacier extents for three dates during the 20th century. The 1906 extent is derived from the documents of the Duce of Abruzzi's expedition, the 1955 extent is from a detailed map made from vertical aerial photographs (D.O.S., 1962), and the 1990 status is mainly based on two Innsbruck University expeditions (Kaser and Nogglér, 1991, 1996). Data of glacier extents for the minor glaciated mountains in the Rwenzori Range, Mount Emin, Gessi, and Luigi di Savoia, are not known exactly and, thus, are excluded from this investigation.

According to their different area altitude distributions, the glaciers on the individual mountains of the Central Rwenzori Range have retreated diversely until the early 1990s (Table I): Mount Stanley could at least keep 35% of its glacier surface area of 1906, Mount Speke 25%, and Mount Baker only kept 8% (Kaser and Osmaston, 2002). Besides the generally strong recession, the complex retreat pattern, which is particularly conspicuous on the single glaciers Speke and Moore (emphasized in Figure 2), is striking and calls for a closer examination. First, it must be recognized that these glaciers' western sections, which are exposed to the morning sun, have receded much more than their eastern sections, which are shaded by the relief in the morning hours. Second, a prominent loss in the upper parts of these glaciers has also occurred. How can the differential retreat of Speke and Moore Glaciers be explained?

A conceptual approach, based on the observed phenomena, is as follows. The obvious loss of accumulation area indicates a strong reduction of accumulation and, thus, a decay of ice dynamics. Consequently, the mass balance in the lower parts of the glaciers is dominated by ablation; compensation through ice advection is missing. Potential spatial differences in ablation lead to spatially differential ice wastage. The only considerable energy for ablation, which can be subject to spatial differences in complex terrain, is provided by incoming shortwave radiation, since the albedo of the glacier surface cannot maintain the same pattern over a long period (especially not in tongue areas). Changes in incoming shortwave radiation exclusively depend on cloudiness, and cloudiness depends on the relative humidity of the air. The Speke and Moore Glaciers' marked retreat in

Table I. The reconstructed glacier surface areas of Mount Baker, Mount Speke, Mount Stanley, and (as the sum) of the Central Rwenzori Range as absolute values ( $A(\text{km}^2)$ ) and relative values to the surface area in 1906 ( $A(\%)$ ). (From Kaser (1996))

	1906		1955		1990	
	$A(\text{km}^2)$	$A(\%)$	$A(\text{km}^2)$	$A(\%)$	$A(\text{km}^2)$	$A(\%)$
Mount Baker	1.468	100	0.617	42	0.120	8
Mount Speke	2.187	100	1.306	60	0.555	25
Mount Stanley	2.854	100	1.885	66	0.999	35
Central Rwenzori (total)	6.509	100	3.808	58	1.674	26

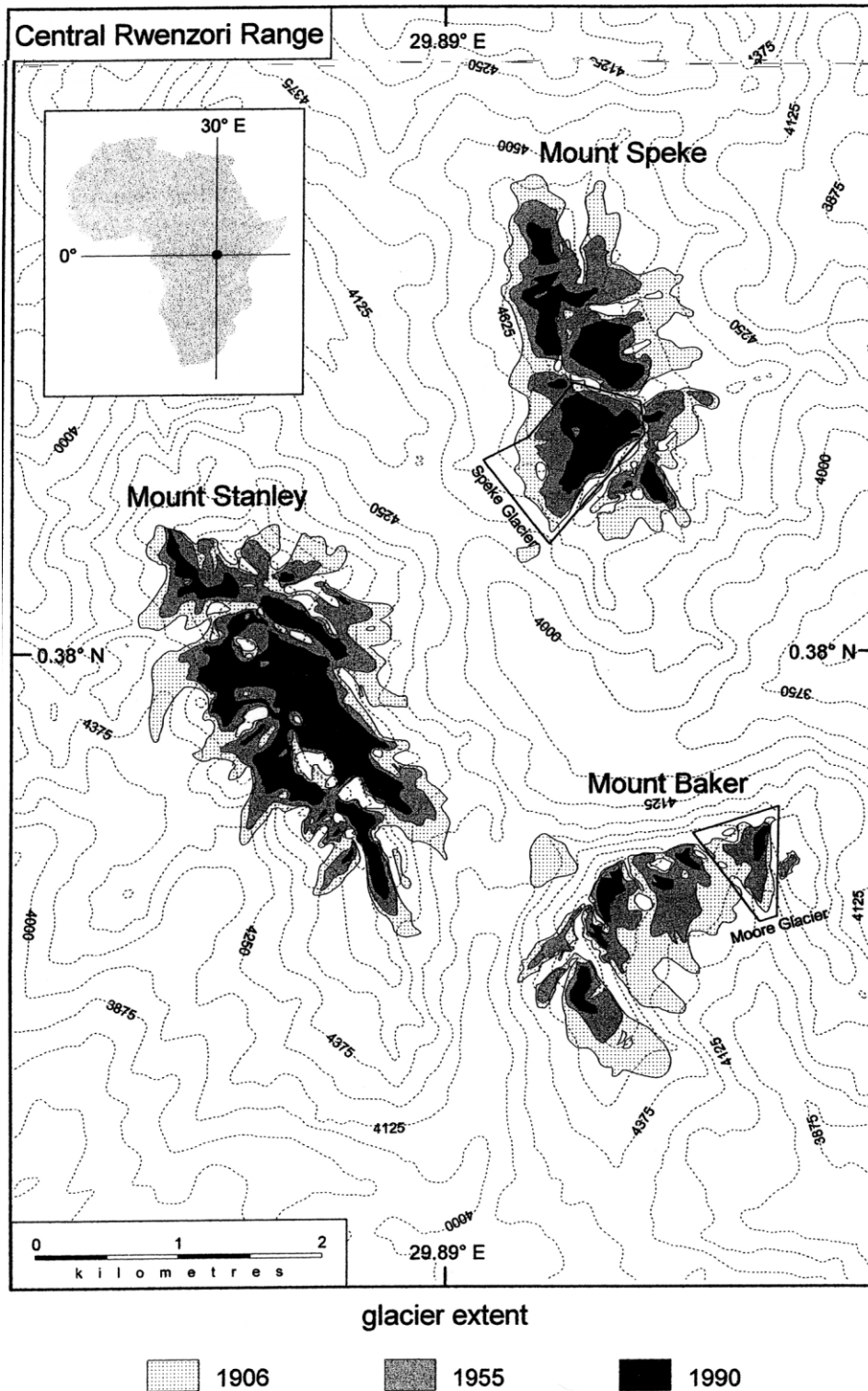


Figure 2. The reconstructed glacier surface areas of Mount Baker, Mount Speke, and Mount Stanley 1906, 1955, and 1990 (contours in metres, as calculated from the original values in feet/equidistance 125 m). Base map by D.O.S. (1962); (after Kaser and Osmaston (2002))

their morning-sun-exposed western sections, found in all altitude spans, evokes the hypothesis of a later onset of convective cloudiness in the morning hours and, therefore, an increase in incoming shortwave radiation. This, in turn, is related to generally drier conditions, compared with those that led to the last maximum extent of East African glaciations. Drier conditions during the 20th century agree with the initially postulated reduction in accumulation and, furthermore, with the knowledge of modern climate fluctuations in East Africa as outlined in Section 1. It is the aim of this study (i) to quantify the increase in incoming shortwave radiation due to a change in onset of convective cloudiness during the morning hours, and (ii) to evaluate the hypothesis of increased incoming shortwave radiation as the reason for the complex retreat patterns by quantifying the correlation between increased incoming shortwave radiation and glacier recession for the entire Central Rwenzori Range.

### 3. THE MODELLING PROCESS

Based on the Geo Information Systems Arc/Info and ArcView GIS, modelling incoming shortwave radiation was chosen as the methodology for this investigation. A digital terrain model (DTM) was constructed from the 1955 map of the Central Rwenzori Range (D.O.S., 1962) and saved as a grid with a cell size of 25 m. More details on the DTM construction (e.g. interpolation algorithm, software) can be found in Mölg (2001, 2002). The climatological modelling process consists of two steps: (i) formulation of a radiation model and its combination with the DTM (Section 3.1), and (ii) definition of two different scenarios that refer to the two climatic regimes of East Africa in question (Section 3.2).

#### 3.1. The radiation model

The radiation model presented in this section is a modified version of the model used by Hastenrath and coworkers (Hastenrath, 1984; Kruss and Hastenrath, 1987; Hastenrath and Kruss, 1988; Hastenrath and Greischar, 1997) modelling incoming shortwave radiation on Mount Kenya and Kilimanjaro. The basic part of the radiation model is the parameterization for calculating the clear-sky direct solar radiation  $SW\downarrow (dir)$  on a planar surface and was initially presented by Bernhardt and Philipps (1958). This formula can be written as

$$SW\downarrow (dir) = S_0 E_0 \cos \zeta_p \left[ \frac{0.907}{(\sin h)^{0.018}} \right]^{T/\sin h} \quad (1)$$

where  $S_0$  is the solar constant ( $1370 \text{ W m}^{-2}$ ),  $E_0$  is the eccentricity correction factor,  $\zeta_p$  is the zenith angle of the sun with respect to an arbitrarily oriented and inclined plane,  $h$  is the solar elevation and  $T$  is the so-called Linke turbidity factor. The eccentricity correction factor  $E_0$ , which is the square of the ratio of the mean to the true distance of the sun ( $r_0/r$ ), can be calculated from (Iqbal, 1983):

$$E_0 = (r_0/r)^2 = 1.000\ 110 + 0.034\ 221 \cos \Gamma + 0.001\ 28 \sin \Gamma \\ + 0.000\ 719 \cos(2\Gamma) + 0.000\ 077 \sin(2\Gamma) \quad (2)$$

$\Gamma$  symbolizes the day angle and can be obtained from the following formula in degrees:

$$\Gamma = 360(n - 1)/365 \quad (3)$$

where  $n$  is the day number of the year, ranging from 1 (1 January) to 365 (31 December). February is always assumed to have 28 days. The zenith angle of the sun with respect to an arbitrarily oriented and inclined plane  $\zeta_p$  was computed using (Iqbal, 1983):

$$\cos \zeta_p = (\cos \beta \sin \varphi - \cos \varphi \cos \alpha \sin \beta) \sin \delta + (\sin \varphi \cos \alpha \sin \beta + \cos \beta \cos \varphi) \cos \delta \cos \omega \\ + \sin \alpha \sin \beta \cos \delta \sin \omega \quad (4)$$

The angle  $\alpha$  describes the azimuth angle of the plane, i.e. the deviation of the normal to the surface with respect to the local meridian (east positive, west negative);  $\beta$  is the slope of the plane. Both angles can be determined from the DTM for each cell. The Central Rwenzori Range's latitude  $\varphi$  was set to 0.38. The angle  $\omega$  symbolizes the hour angle of the sun (noon zero, morning positive, afternoon negative) and finally  $\delta$  is the solar declination, which is presented by the following expression in degrees (Iqbal, 1983):

$$\delta = [0.006\,918 - 0.399\,912 \cos \Gamma + 0.070\,257 \sin \Gamma - 0.006\,758 \cos(2\Gamma) + 0.000\,907 \sin(2\Gamma) - 0.002\,697 \cos(3\Gamma) + 0.001\,48 \sin(3\Gamma)]180/\pi \quad (5)$$

$\Gamma$  is again the day angle (Equation (3)), and  $\pi$  is a mathematical constant (3.141 592 6). The term  $[0.907/(\sin h)^{0.018}]^{T/\sin h}$  in Equation (1) describes the extinction of solar radiation, which depends on solar elevation and atmospheric turbidity. Solar elevation  $h$  can be determined from (Robinson, 1966):

$$\sin h = \sin \delta \sin \varphi + \cos \delta \cos \varphi \cos \omega \quad (6)$$

The angles  $\delta$ ,  $\varphi$  and  $\omega$  are again solar declination, latitude, and hour angle of the sun, respectively, as discussed above. The Linke turbidity factor  $T$  is an indicator of the amount of water vapour and haze in the air (Robinson, 1966). Considering the very little dust at high altitude on a tropical mountain (Hastenrath, 1984), the following formula can be used to calculate  $T$  (Bernhardt and Philipps, 1958):

$$T = 1.39 + 0.112e_0 \quad (7)$$

The only parameter, which has to be determined, is the water vapour pressure  $e_0$  (in mm Hg) over the glacier surface. Representative for the climatic environment of the Rwenzori glaciers is saturation at 0°C (Kaser and Osmaston, 2002), which results in a turbidity factor of 1.9.

Under clear-sky conditions the diffuse component of incoming shortwave radiation at high altitude is very small compared with the value of direct solar radiation. Measurements on Mount Kenya show that the diffuse component only accounts for 5% of the clear-sky incoming shortwave radiation (Hastenrath, 1984). Therefore, the value for incoming shortwave radiation under clear sky conditions  $SW\downarrow_0$  was set 5% greater than the value of direct solar radiation calculated from Equation (1). Incoming shortwave radiation under cloudy sky  $SW\downarrow_C$  can be determined from the following parameterization (Budyko, 1974):

$$SW\downarrow_C = SW\downarrow_0 (1 - kC) \quad (8)$$

$SW\downarrow_0$  symbolizes incoming shortwave radiation under clear sky,  $k$  is an empirical coefficient (0.65 at the equator) and  $C$  is cloudiness in tenths.

The radiation model was formulated in Arc/Info's programming language AML (ArcMacro Language) and then combined with the DTM. According to the tropical conditions, calculations were performed between 06:00 and 18:00 true solar time with a temporal resolution of 30 min, including shading by the relief.

### 3.2. The climate scenarios

Incoming shortwave radiation was calculated for two scenarios (A and B) with temporally varying onset of convective cloudiness.

For the less humid climate after 1880, scenario A is based on the observations reported by Whittow (1960), Whittow *et al.* (1963), and Osmaston (1989), which include the annual cycle of air masses and the daily onset of cloudiness. The following characteristics for scenario A are chosen: rainy seasons are from March to May and from August to December with onset of convective cloudiness at 08:30, drier seasons are in January–February and June–July with onset of convective cloudiness at 09:00. In the model, cloud cover starts immediately with 10/10 coverage and lasts until sunset for simplification. Obviously, this does not agree with reality, but it produces the same shading effects as vertically extended clouds rising from

easterly oriented slopes in the morning and intensifying during the day. Generally, the combination of both a pronounced spatial differentiation in incoming shortwave radiation, as based on the cloud conditions in scenario A, and a strongly reduced accumulation could produce the spatial diversity in the glacier retreats. However, the spatial distribution of mean annual incoming shortwave radiation in scenario A does not show a conspicuous differentiation pointing to the differential glacier retreats (Mölg, 2001). Thus, the reduction in accumulation by itself cannot cause the spatial differences in the ice retreat. A further scenario considering a change in cloudiness is demanded.

Scenario B refers to the more humid climate of the couple of decades preceding 1880, when glaciers in East Africa experienced favourable conditions that led to the last maximum extent. There are no comparable observations of these decades, but certainly conditions were more humid than after 1880 (Kruss, 1983, 1984; Hastenrath, 1984, 2001; Nicholson *et al.*, 2000; Nicholson and Yin, 2001). In the model, the higher humidity is expressed by a half-hourly earlier onset of cloudiness in the morning hours: at 08:00 in the rainy seasons and at 08:30 in the drier seasons. Additionally, a prolongation of the rainy seasons of about 1 month per year is included, treated in such a way that each of the two rainy seasons starts 8 days earlier and lasts 8 days longer. The effect of changed cloud conditions on the spatial and temporal distribution of incoming shortwave radiation in the Central Rwenzori Range since *ca* 1880 can now be investigated by subtracting the scenario B results from the scenario A results. A detailed picture of the whole modelling process, including a quality test of the DTM, examples of AML scripts, and an analysis of the basic data for the scenarios, is offered by Mölg (2001).

#### 4. RESULTS AND DISCUSSION

The spatial distribution of increased mean annual incoming shortwave radiation due to a later onset of convective cloudiness and shorter rainy seasons is shown in Figure 3. As expected, a well pronounced contrast between eastern and western slopes of the mountains is found. Averaged over the entire Central Rwenzori Range, the mean annual increase in incoming shortwave radiation amounts to  $7 \text{ W m}^{-2}$  (data range from 0 to  $14.9 \text{ W m}^{-2}$ ). The main contribution to this increase must be attributed to the all-year change in the daily onset of cloudiness, while shorter rainy seasons only affect 32 days of the year, as defined in the model (Section 3.2). It should be mentioned that changing the time span between the onset of cloudiness in the two scenarios, e.g. from 0.5 h to 1 h, does, of course, change the absolute amount of increased incoming shortwave radiation, but it does not change the spatial distribution of the increase in incoming shortwave radiation (Mölg, 2001).

A first general view at Figure 3 indicates the verification of the hypothesis. In particular, on the single glaciers Speke and Moore it can be seen that radiation is enhanced relatively strongly in their western sections where they retreated drastically during the 20th century. Their eastern sections show no or just a small increase in incoming shortwave radiation. Though less pronounced, similar patterns are found on the entire mountains Baker and Speke, where strong glacier area shrinkages correlate with strong increases in incoming shortwave radiation. In contrast to this, the recession of Mount Stanley's glaciation seems to be evenly pronounced in areas of differently increased incoming shortwave radiation.

In order to quantify the correlation between increased incoming shortwave radiation and glacier recession, the following procedure is applied: first, the spatially differentiated pattern of increased mean annual incoming shortwave radiation is classified into two groups, areas of 'no or little increase in mean annual incoming shortwave radiation' ( $0 < 5 \text{ W m}^{-2}$ : category 1), and areas of a 'clear increase in mean annual incoming shortwave radiation' ( $\geq 5 \text{ W m}^{-2}$ : category 2). The separation is based on the frequency distribution, which shows a bimodal shape with a minimum around  $5 \text{ W m}^{-2}$ . In the second step, the classified pattern of increased incoming shortwave radiation and the spatial pattern of glacier retreats are overlaid. The Semper Glacier is not considered in this quantification because its retreat and disappearance in the early 1940s is the result of a change in mechanical accumulation processes. This glacier was fed by snow drifting over the summit ridge of Mount Baker, and with the shrinkage of the upper parts of East Baker Glacier this source was cut off (Osmaston, 1989).

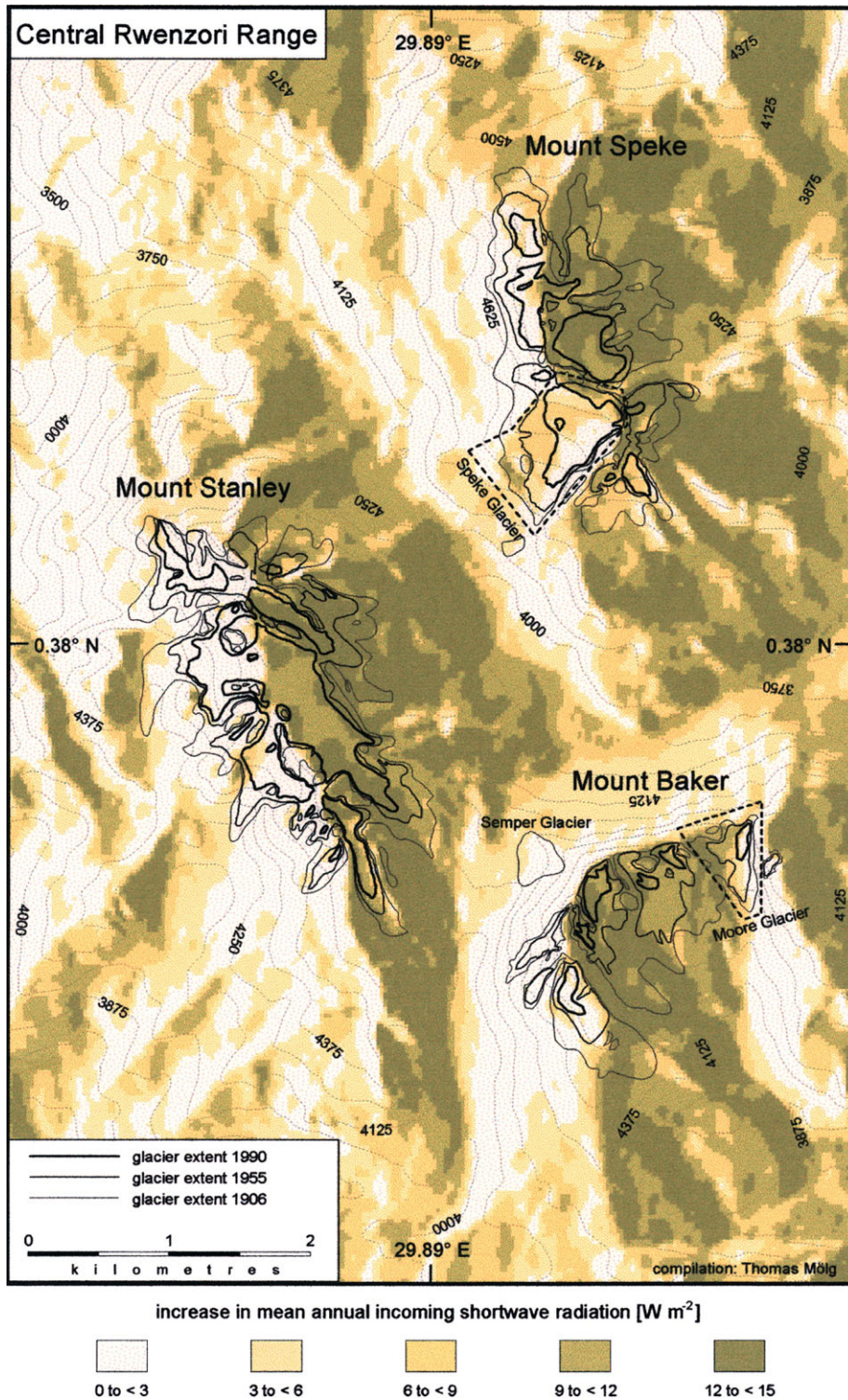


Figure 3. Mean annual increase in incoming shortwave radiation since ca 1880 (scenario A – B) in the Central Rwenzori Range (contours in metres, as calculated from the original values in feet/equidistance 125 m)

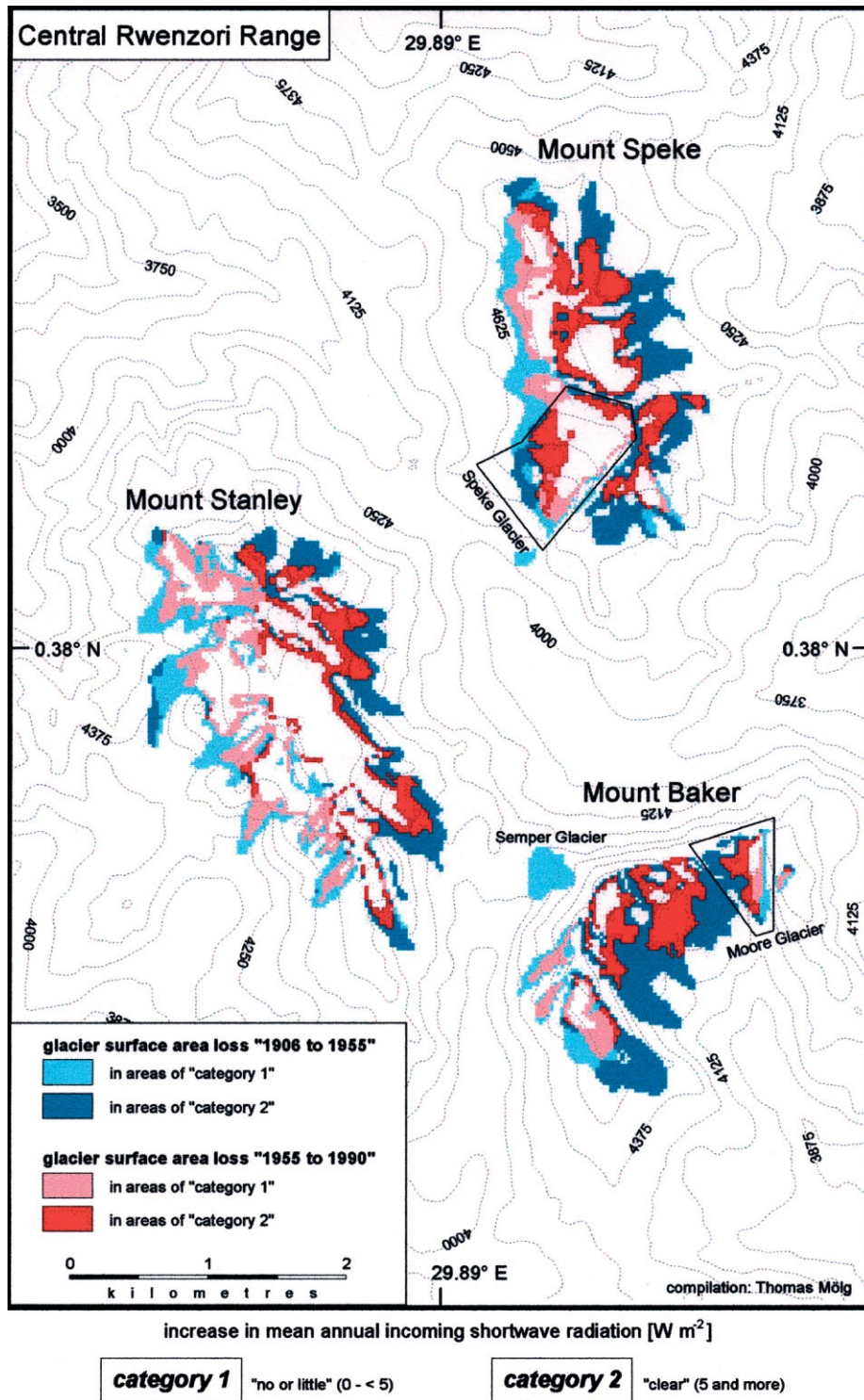


Figure 4. Glacier surface area loss in areas of 'no or little increase' ( $0 < 5 W m^{-2}$ ; category 1) and in areas of a 'clear increase' ( $\geq 5 W m^{-2}$ ; category 2) in mean annual incoming shortwave radiation in the Central Rwenzori Range in the periods 1906 to 1955 and 1955 to 1990 (contours in metres, as calculated from the original values in feet/equidistance 125 m)

The result of the overlay is shown in Figure 4. The two black hues define glacier surface loss in areas of 'clearly increased incoming shortwave radiation' (category 2), grey hues the loss in areas of 'no or little increase in incoming shortwave radiation' (category 1). The lighter hue of the blacks and greys indicates that the loss happened in the period 1906–55, the darker hue refers to the period 1955–90. (For the online version of this figure: blue symbolizes glacier surface area loss in the period 1906–1955, red refers to the period 1955–90; light hues denote that glaciers retreated in areas of 'no or little increase in incoming shortwave radiation' (category 1), dark hues pick out glacier surface area loss in regions of 'clearly increased incoming shortwave radiation' (category 2)). This graphic is numerically supported by the values given in Table II. Viewing the mountains Baker and Speke, the qualitative interpretations of Figure 3 are quantitatively confirmed by both Figure 4 and Table II. Glacier surface area loss in the two periods examined is more than twice as high in areas of category 2 as in areas of category 1. The individual glaciers Speke and Moore, which are located in these two mountains, fit well into this picture (Table II). On Mount Stanley, in contrast, glacier surface area loss in the two different categories is approximately equal in both periods of time (Table II). Finally, the question of the behaviour of the entire glaciation in the Central Rwenzori Range arises. During the first half of the 20th century, glacier surface area loss in regions of category 2 is approximately twice as high as in areas of category 1 (Table II). The plain ratio between category 1 and category 2 is maintained but weakens in the second half of the 20th century, denoting that the influence of ablation caused by shortwave radiation decreased. In its essential features, this aspect agrees with the findings of Hastenrath and Kruss (1992) for Mount Kenya. There, the authors assigned the retreat of the glaciers in the first half of the 20th century to shortwave radiation, and the retreat between 1963 and 1987 primarily to a combination of a 0.2 K warming and an increase in specific humidity of 0.3 g kg<sup>-1</sup>.

The explanation for the divergent behaviour of Mount Stanley's glaciation, compared with the glaciers of Mount Baker and Mount Speke, may be found in the hypsographic curves of the glaciations of the respective mountains (Figure 5). The equilibrium line altitude (ELA<sub>St</sub>) drawn in Figure 5 was determined by Kaser and Osmaston (2002) for Mount Stanley's glaciation around 1955 in a hypothetically steady-state condition and, according to theoretical considerations for tropical conditions, applying an accumulation area ratio of 0.8. However, because the glaciers of the Rwenzori had not been in equilibrium but under strong recession, the real ELA must clearly have been higher than marked in Figure 5 (*ca* 4900 m). This leads to the assumptions that Mount Baker and Mount Speke had no accumulation area during the 20th century and that an effective accumulation input can only be expected on Mount Stanley. Although increased incoming shortwave radiation caused spatially differential glacier retreats on the Baker and Speke mountains, intact accumulation and ice advection on Mount Stanley could partially compensate this radiationally caused ablation. Ice recession on Mount Stanley, therefore, was limited to the tongue areas, whereas Mount Baker and Mount Speke lost ice volume in all altitude spans. Determining glacier average mean annual incoming shortwave radiation

Table II. Relative loss of glacier surface area in areas of 'no or little increase' ( $0 < \Delta W m^{-2}$ : category 1) and in areas of a 'clear increase' ( $\geq 5 W m^{-2}$ : category 2) in mean annual incoming shortwave radiation on Mount Baker, Mount Speke, Mount Stanley, of Speke and Moore Glaciers, and (as a whole) in the Central Rwenzori Range in the periods 1906 to 1955 and 1955 to 1990

	1906 to 1955 (%)		1955 to 1990 (%)	
	Category 1	Category 2	Category 1	Category 2
Mount Baker	18.2	81.8	30.7	69.3
Mount Speke	29.3	70.7	28.8	71.2
Mount Stanley	47.4	52.6	52.3	47.7
Speke Glacier	35.5	64.5	32.2	67.8
Moore Glacier	32.5	67.5	28.9	71.1
Central Rwenzori (total)	32.7	67.3	39.1	60.9

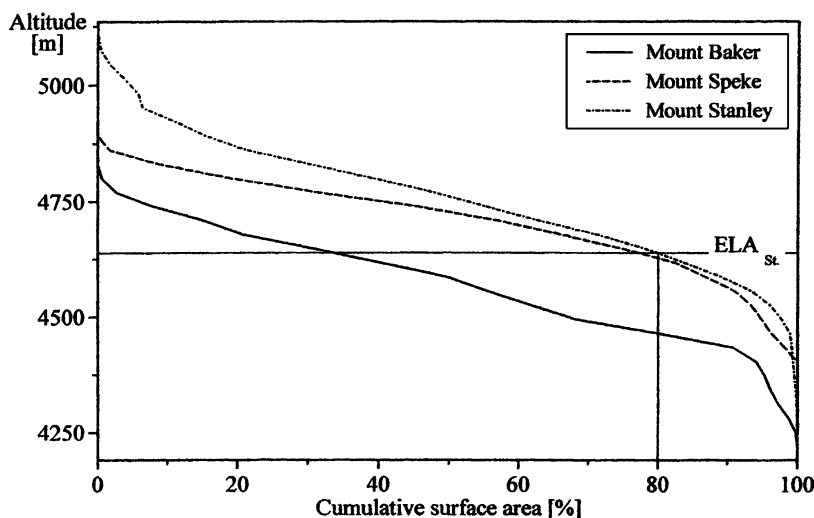


Figure 5. Hypsographic curves of the glaciations of Mount Baker, Mount Speke, and Mount Stanley 1955 (ELA<sub>St</sub>: equilibrium line altitude on Mount Stanley in a hypothetically steady-state condition, determined by an accumulation area ratio (AAR) of 0.8); (modified from Kaser and Osmaston (2002))

in scenario A (referring to the conditions of the relatively dry climatic regime after *ca* 1880) supports this explanation. Mount Baker's and Mount Speke's glaciations retreated to more protected areas during the 20th century, whereas Mount Stanley's glaciation continuously receded to even less radiationally protected areas (Mölg, 2001). These time series point to the fact that incoming shortwave radiation has a smaller influence on glacier area loss on Mount Stanley, since its relative glacier recession is the least within the Central Rwenzori Range's mountains.

## 5. SUMMARY AND CONCLUSIONS

Complex retreat patterns of the glaciers in the Rwenzori Range, which are particularly obvious on the single glaciers Speke and Moore, evoked — in connection with the information on an abrupt change to drier conditions in East Africa around 1880 — the hypothesis of increased incoming shortwave radiation due to a change in the diurnal cycle of convective cloudiness. Modelling changes in incoming shortwave radiation shows that a later onset of cloudiness in the morning hours and shorter rainy seasons, accompanying the drier conditions, lead to a spatially differential increase in incoming shortwave radiation that shows a direct proportionality to glacier recession. Glacier surface area loss in the entire Central Rwenzori Range between 1906 and 1955 was twice as high in areas of a 'clear increase in mean annual incoming shortwave radiation' ( $\geq 5 \text{ W m}^{-2}$ ) as in areas of 'no or little increase in mean annual incoming shortwave radiation' ( $0 < 5 \text{ W m}^{-2}$ ). This plain picture remains in the second half of the 20th century between 1955 and 1990. Glacier surface area loss in regions of 'clearly increased incoming shortwave radiation' is 1.6 times the amount of the loss in areas of 'no or little increase in incoming shortwave radiation'. The spatial distribution of the absolute amounts of mean annual incoming shortwave radiation during the 20th century cannot explain the differential glacier retreats, which supports the change in cloudiness. The diverging behaviour of Mount Stanley's glaciation — a rather uniform glacier surface area loss in the two defined categories — seems to be an effect of its still intact accumulation, which can, at least partially, compensate the ablation caused by increased incoming shortwave radiation. In contrast, accumulation on the mountains Baker and Speke disappeared during the 20th century.

The results confirm the hypothesis of increased incoming shortwave radiation as the reason for the complex and spatially differential glacier retreat in the Rwenzori mountains. In the context of modern climate fluctuations, the results of this study support the findings of Kruss (1983, 1984), Hastenrath (1984, 2001),

Nicholson *et al.* (2000), and Nicholson and Yin (2001); a climatic change in East Africa was concentrated at the end of the 19th century, leaving a humid regime behind and leading to a relatively dry regime, which is forcing the recession of glaciers not only by less accumulation but also — as made clear in this paper — by less protection against shortwave radiation through clouds. A steadily increasing air temperature cannot hold for the spatial differences. It can only support the general trend of glacier recession, affecting both a generally increased ablation and a higher position of the lower snow fall limit.

## NOTE

1. The spelling was agreed to be Rwenzori at the Rwenzori Conference 1996 (Osmaston *et al.*, 1998).

## REFERENCES

- Bernhardt F, Philipps H. 1958. *Die räumliche und zeitliche Verteilung der Einstrahlung, der Ausstrahlung und der Strahlungsbilanz im Meeresniveau, Teil 1: Die Einstrahlung*. Meteorologischer und Hydrologischer Dienst der DDR: Berlin.
- Budyko MI. 1974. *Climate and Life*. Academic Press: New York, London.
- D.O.S. 1962. *Central Rwenzori 1 : 25.000*. Directorate of Overseas Surveys: Entebbe.
- Griffiths JF. 1972. *Climates of Africa*. Elsevier: Amsterdam, London, New York.
- Hastenrath S. 1984. *The Glaciers of Equatorial East Africa*. Reidel: Dordrecht, Boston, Lancaster.
- Hastenrath S. 1989. Ice flow and mass changes of Lewis Glacier, Mount Kenya, East Africa: observations 1974–86, modelling, and predictions to the year 2000. *Journal of Glaciology* **35**: 325–331.
- Hastenrath S. 1991. *Climate Dynamics of the Tropics*. Kluwer: Dordrecht, Boston, London.
- Hastenrath S. 1995. Glacier recession on Mount Kenya in the context of the global tropics. *Bulletin d'Institut Français Études Andines* **24**: 633–638.
- Hastenrath S. 2001. Variations of East African climate during the past two centuries. *Climatic Change* **50**: 209–217.
- Hastenrath S, Greischar L. 1997. Glacier recession on Kilimanjaro, East Africa, 1912–89. *Journal of Glaciology* **43**: 455–459.
- Hastenrath S, Kruss PD. 1988. The role of radiation geometry in the climate response of Mount Kenya's glaciers, part 2: sloping versus horizontal surfaces. *International Journal of Climatology* **8**: 629–639.
- Hastenrath S, Kruss PD. 1992. The dramatic retreat of Mount Kenya's glaciers between 1963 and 1987: greenhouse forcing. *Annals of Glaciology* **16**: 127–133.
- Hastenrath S, Rostom R, Caukwell RA. 1989. Variations of Mount Kenya's glaciers 1963–87. *Erdkunde* **43**: 202–210.
- Iqbal M. 1983. *An Introduction to Solar Radiation*. Academic Press: Toronto, New York, London.
- Kaser G. 1999. A review of the modern fluctuations of tropical glaciers. *Global and Planetary Change* **22**: 93–103.
- Kaser G. 2001. Glacier–climate interactions at low latitudes. *Journal of Glaciology* **47**: 195–204.
- Kaser G, Noggler B. 1991. Observations on Speke Glacier, Rwenzori Range, Uganda. *Journal of Glaciology* **37**: 313–318.
- Kaser G, Noggler B. 1996. Glacier fluctuations in the Rwenzori Range (East Africa) during the 20th century — a preliminary report. *Zeitschrift für Gletscherkunde und Glazialgeologie* **32**: 109–117.
- Kaser G, Osmaston H. 2002. *Tropical Glaciers*. Cambridge University Press: Cambridge.
- Kaser G, Hastenrath S, Ames A. 1996. Mass balance profiles on tropical glaciers. *Zeitschrift für Gletscherkunde und Glazialgeologie* **32**: 75–81.
- Kruss PD. 1983. Climate Change in East Africa: a numerical simulation from the 100 years of terminus record at Lewis Glacier, Mount Kenya. *Zeitschrift für Gletscherkunde und Glazialgeologie* **19**: 43–60.
- Kruss PD. 1984. Terminus response of Lewis Glacier, Mount Kenya, to sinusoidal net balance forcing. *Journal of Glaciology* **30**: 212–217.
- Kruss PD, Hastenrath S. 1987. The role of radiation geometry in the climate response of Mount Kenya's glaciers, part 1: horizontal reference surfaces. *International Journal of Climatology* **7**: 493–505.
- Mölg T. 2001. *Modellierung der Globalstrahlung in Zusammenhang mit neuzeitlichen Gletscherschwankungen am Rwenzori*. Master's thesis, University of Innsbruck, Innsbruck.
- Mölg T. 2002. Modellierung der kurzwelligen Einstrahlung mit GIS am Beispiel eines tropischen Hochgebirges. In *Beiträge zum AGIT-Symposium Salzburg 2002*, Strobl J, Blaschke T, Griesebner G (eds). Wichmann: Berlin, Heidelberg, 347–356.
- Nicholson SE, Yin X. 2001. Rainfall conditions in Equatorial East Africa during the nineteenth century as inferred from the record of Lake Victoria. *Climatic Change* **48**: 387–398.
- Nicholson SE, Yin X, Ba MB. 2000. On the feasibility of using a lake water balance model to infer rainfall: an example from Lake Victoria. *Hydrological Sciences Journal—Journal des Sciences Hydrologiques* **45**: 75–95.
- Osmaston H. 1989. Glaciers, glaciations and equilibrium line altitudes on the Rwenzori. In *Quaternary and Environmental Research on East African Mountains*, Mahaney WC (ed.). Balkema: Rotterdam: 31–104.
- Osmaston H, Tukahirwa J, Basalirwa C, Nyakaana J (eds). 1998. *The Rwenzori Mountains National Park, Uganda*. Makerere University: Kampala.
- Robinson N (ed.). 1966. *Solar Radiation*. Elsevier: Amsterdam, London, New York.
- Thompson LG, Mosley-Thompson E, Davis ME, Henderson KA, Brecher HH, Zagorodnov VS, Mashiotta TA, Lin PN, Mikhaleiko VN, Hardy DR, Beer J. 2002. Kilimanjaro ice core records: evidence of Holocene climate change in tropical Africa. *Science* **298**: 589–593.
- Troll C, Wien K. 1949. Der Lewis Gletscher am Mount Kenia. *Geografiska Annaler* **31**: 257–274.
- Wagnon P, Ribstein P, Francou B, Sicart JE. 2001. Anomalous heat and mass budget of Glacier Zongo, Bolivia, during the 1997/98 El Niño year. *Journal of Glaciology* **47**: 21–28.

- Weischet W, Endlicher W. 2000. *Regionale Klimatologie, Teil 2: Die Alte Welt (Europa, Afrika, Asien)*. Teubner: Stuttgart, Leipzig.
- Whittow JB. 1960. Some observations on the snowfall of Rwenzori. *Journal of Glaciology* **3**: 765–772.
- Whittow JB, Shepherd A, Goldthorpe JE, Temple PH. 1963. Observations on the glaciers of the Rwenzori. *Journal of Glaciology* **4**: 581–616.